Journal of Solid Mechanics Vol. 1, No. 4 (2009) pp. 328-342

Effects of Geometric Nonlinearity on Stress Analysis in Large Amplitude Vibration of Moderately Thick Annular Functionally Graded Plate

M.H. Amini*, A. Rastgoo, M. Soleimani

Faculty of Mechanical Engineering, College of Engineering, University of Tehran, Tehran, Iran

Received 25 August 2009; accepted 16 December 2009

ABSTRACT

This paper deals with the nonlinear free vibration of thick annular functionally graded material plates. The thickness is assumed to be constant. Material properties are assumed to be graded in the thickness direction according to a simple power law distribution in terms of the volume fractions of the constituents. The formulations are based on the first-order shear deformation plate theory and von Kármán-type equation. For harmonic vibrations, by using assumed-time-mode method sinusoidal oscillations are assumed, then the time variable is eliminated by applying Kantorovich averaging method. Thus, the basic governing equations for the problem are reduced to a set of ordinary differential equations in term of radius. The results reveal that vibration amplitude and volume fraction have significant effects on the resultant stresses in large amplitude vibration of the functionally graded thick plate.

Keywords: Functionally graded material; Large amplitude vibration; Stress analysis; Thick annular plate

1 INTRODUCTION

CIRCULAR and annular plates are used in many engineering applications. Such structures are often subjected to severe dynamic loading conditions and can exhibit large amplitude vibrations of the order of the plate thickness. In this case a significant geometrical nonlinearity is induced. Numerous studies on free and forced vibration for isotropic and composite multilayered plates with or without initial thermal and or mechanical in-plane loads have been reported [1- 6]. Xuefeng et al. [7] presented the coupled thermoelastic free vibration of clamped circular plate. Galerkin's method has been used to drive the nonlinear differential equations. Arafat et al. [8] studied the behavior of annular plates with clamped–clamped immovable edges subjected to axisymmetric in-plane thermal loads. A numerical shooting method is used to calculate the mode shapes and natural frequencies.

Functionally graded materials (FGMs) are inhomogeneous composite materials and are made from different phases of materials such as ceramic and metal. FGMs have different applications especially for space vehicles, automobile, defense industries, electronics, and biomedical sectors. FGMs properties vary continuously from one interface to the other. Those are achieved by gradually varying volume fraction of constituent materials. In recent years, the nonlinear vibration of FGM plates has attracted increasing research efforts. Amini et al. [9] studied the three-dimensional free vibration of FGM plates resting on an elastic foundation. Governing equations were based on linear, small-strain and three-dimensional elasticity theory and Chebyshev polynomials and Ritz's method were employed to solve the equations. Ebrahimi et al. [10] presented a theoretical solution for free vibration of moderately thick shear deformable annular functionally graded plate coupled with piezoelectric layers based on

* Corresponding author. Tel.: +98 21 2284 8984.
E-mail address: mhamini@ut.ac.ir (M.H. Amini).

Mindlin's plate theory. Praveen and Reddy [11] analyzed the nonlinear static and dynamic response of functionally graded ceramic–metal plates in a steady temperature field and subjected to dynamic transverse loads by the finite element method (FEM) based on the first-order shear deformation plate theory (FSDPT). Reddy [12] developed both theoretical and finite element formulations for thick FGM plates according to the higher-order shear deformation plate theory (HSDPT), and studied the nonlinear dynamic response of FGM plates subjected to suddenly applied uniform pressure. Woo and Meguid [13] investigated the nonlinear analysis of functionally graded plates and shallow shells. An analytical solution has been provided for the coupled large deflection of plates and shallow shells under mechanical load and temperature field, and the solution has been obtained in terms of Fourier series. Woo et al. [14] derived an analytical solution for the nonlinear free vibration behavior of thin rectangular functionally graded plates. Allahverdizade et al. [15] studied the effects of large vibration amplitudes on the stresses of thin circular functionally graded plates. Kitipornchai et al. [16] presented a semi-analytical solution for nonlinear vibration of laminated FGM plates with geometric imperfections and showed that the vibration frequencies are very much dependent on the vibration amplitude and the imperfection mode. They [17] also studied the random vibration of the functionally graded laminates with third-order shear deformation plate theory and general boundary conditions in thermal environments.

The aim of this present paper is to study nonlinear free vibration of thick annular FGM plate. Material properties are assumed to be graded in the thickness direction according to a simple power law distribution in terms of the volume fractions of the constituents. The formulations are based on the first-order shear deformation plate theory and von Kármán-type equation. For harmonic vibrations, by using assumed-time-mode method sinusoidal oscillations are assumed, then the time variable is eliminated by applying Kantorovich averaging method. Thus, the basic governing equations for the problem are reduced to a set of ordinary differential equations. Extensive numerical results are presented in both dimensionless tabular and graphical forms, and highlight the influence of material composition and vibration amplitude on induced stresses in large amplitude vibration of annular FGM plate.

2 THEORETICAL FORMULATIONS

2.1 Functionally graded materials (FGM)

Consider an annular FGM plate of constant thickness h and inner and outer radius r_i and r_o respectively (Fig. 1), which is made from a mixture of ceramic and metal and the composition varies from the top to the bottom surface, i.e., the top surface $z = h/2$ of the plate is ceramic-rich whereas the bottom surface $z = -h/2$ is metal-rich. In such a way, an arbitrary material property P (e.g., Young's modulus E, and mass density ρ) of the functionally graded plate is assumed to vary through the thickness of the plate, as a function of the volume fraction and properties of the constituent materials as

$$P = P_c V_c + P_m V_m \tag{1}$$

in which V_c and V_m are the ceramic and metal volume fractions and are related by

$$V_c + V_m = 1 \tag{2}$$

For a plate with uniform thickness h and a reference surface at its middle surface, the volume fraction V_c follows a simple power law as [11]

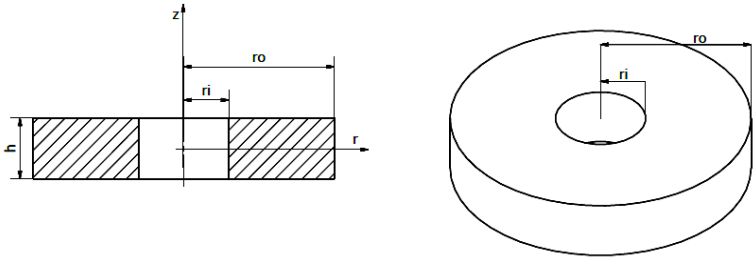

Fig 1.
Geometry and co-ordinates of the plate.

Table 1
Material properties

Material	Property		
	E (GPa)	ρ (kg/m^3)	ν
Aluminum	70	2707	0.3
Alumina	380	3800	0.3

$$V_c = \left(\frac{2z+h}{2h}\right)^g \qquad g \geq 0 \tag{3}$$

Volume fraction index *g* (gradient index) dictates the material variation profile across the plate thickness. It is assumed that the effective Young's modulus E and mass density ρ vary along the thickness, Poisson's ratio v is considered to be constant. From Eqs. (1)– (3), one has [11, 18]

$$P_z = (P_c - P_m)\left(\frac{2z+h}{2h}\right)^g + P_m \tag{4}$$

In Eq. (4) If g= 0 then the plate reduces to a pure ceramic plate (alumina). As the volume fraction index g increases, the ceramic volume fraction decreases until for large enough amount of g material properties tend to pure metal (aluminum). Typical values for alumina and aluminum are listed in Table 1 [19].

2.2 Governing equation

Consider an annular FGM plate located in its initially un-deformed configuration. As usual, the cylindrical coordinate r, θ and z system has its origin at the center of the plate on the middle plane. The r-coordinate direction is radially outward from the center, the z-coordinate is along the thickness, and the θ-coordinate is directed along a circumference of the plate. The plate has uniform thickness h, inner radius r_i and outer radius r_o . (Fig. 1)

For first time, Mindlin [20] represented a new plate theory called "First Order Shear Deformation Theory" in which the effect of shear deformation was not neglected. Consequently, straight material lines that are perpendicular to the mid-plane in the un-deformed state remain straight in the deformed state even though they may not remain perpendicular to the mid-plane. According to this theory, the displacement fields of the plate in the cylindrical coordinate are given as

$$u_r = u(r,t) + z\psi_r(r,t) \tag{5}$$

$$u_z = w(r,t) \tag{6}$$

where u_z and u_r are the displacements in the transverse z-direction and radial r-direction of the plate, respectively; $w(r,t)$ is the transverse displacement and $u(r,t)$ is the radial displacement of the mid-plane; and ψ_r is the rotations of vertical lines perpendicular to the mid-plane, measured on the z–r planes.

The strains for FGM plate at any level z are obtained by substituting the displacement field in the von Karman nonlinear strain-displacement relations [21]

$$\varepsilon_{rr} = \frac{\partial u}{\partial r} + z\frac{\partial \psi_r}{\partial r} + \frac{1}{2}\left(\frac{\partial w}{\partial r}\right)^2 \tag{7}$$

$$\varepsilon_{\theta\theta} = \frac{u}{r} + \frac{z}{r}\psi_r + \frac{1}{2r^2}\left(\frac{\partial w}{\partial \theta}\right)^2 \tag{8}$$

$$\gamma_{rz} = \psi_r + \frac{\partial w}{\partial r} \tag{9}$$

where ε_{rr} and $\varepsilon_{\theta\theta}$ are the normal strains along the r and θ directions and γ_{rz} is the shear strain along z direction acting on a surface with normal parallel to r direction. In terms of Hooke's laws, the normal and shear stresses are given by

$$\sigma_{rr} = \frac{E(z)}{1-\nu^2}(\varepsilon_{rr} + \nu\varepsilon_{\theta\theta}) \tag{10}$$

$$\sigma_{\theta\theta} = \frac{E(z)}{1-\nu^2}(\varepsilon_{\theta\theta} + \nu\varepsilon_{rr}) \tag{11}$$

$$\tau_{rz} = \frac{E(z)}{2(1+\nu)}\gamma_{rz} \tag{12}$$

where

$$E(z) = (E_c - E_m)\left(\frac{2z+h}{2h}\right)^g + E_m \tag{13}$$

The resultant moments, membrane and shear forces are defined as

$$(M_r, M_\theta) = \int_{-h/2}^{h/2} (\sigma_{rr}, \sigma_{\theta\theta}) z \, \mathrm{d}z \tag{14}$$

$$(N_r, N_\theta) = \int_{-h/2}^{h/2} (\sigma_{rr}, \sigma_{\theta\theta}) \, \mathrm{d}z \tag{15}$$

$$Q_r = \kappa \int_{-h/2}^{h/2} \tau_{rz} \, \mathrm{d}z \tag{16}$$

Now by substituting Eqs. (5)–(13) into Eqs. (14)–(16) and integrating, the resultant moments, membrane and shear forces can be expressed as follows

$$N_r = K_1\left(\nu\frac{u}{r} + u_{,r} + \frac{1}{2}(w_{,r})^2\right) + K_2\left(\nu\frac{\psi_r}{r} + \psi_{r,r}\right) \tag{17}$$

$$N_\theta = K_1\left(\frac{u}{r} + \nu u_{,r} + \frac{\nu}{2}(w_{,r})^2\right) + K_2\left(\frac{\psi_r}{r} + \nu\psi_{r,r}\right) \tag{18}$$

$$M_r = K_2\left(\nu\frac{u}{r} + u_{,r} + \frac{1}{2}(w_{,r})^2\right) + K_3\left(\nu\frac{\psi_r}{r} + \psi_{r,r}\right) \tag{19}$$

$$M_\theta = K_2\left(\frac{u}{r} + \nu u_{,r} + \frac{\nu}{2}(w_{,r})^2\right) + K_3\left(\frac{\psi_r}{r} + \nu\psi_{r,r}\right) \tag{20}$$

$$Q_r = \frac{\kappa(1-\nu)}{2}K_1(w_{,r} + \psi_r) \tag{21}$$

The coefficients $K_i (i = 1..3)$ are given in Appendix A. κ is the shear correction factor in Mindlin [20] plate model which is chosen here as 5/6 [21].

By using the Hamilton's principle, governing equations for nonlinear vibration of the first-order plates in cylindrical coordinate can be expressed as follows. Since the principal vibrations take place in the direction perpendicular to the middle plane, it is reasonable to neglect the longitudinal and rotary inertias.

$$(rN_r)_{,r} - N_\theta = 0 \tag{22}$$

$$(rN_r w_{,r})_{,r} + (rQ_r)_{,r} + rP(r,t) = r \cdot I \cdot w_{,tt} \tag{23}$$

$$(rM_r)_{,r} - M_\theta - rQ_r = 0 \tag{24}$$

where $P(r,t)$ is the uniformly distributed lateral loading intensity and I is the transverse inertia which is given in Appendix A. Combining Eqs. (17) – (21) and (22), (23) and (24) one can obtain

$$K_1\left(\frac{(1-\nu)}{2r}(w_{,r})^2 + w_{,rr}w_{,r} + u_{,rr} + \frac{u_{,r}}{r} - \frac{u}{r^2}\right) + K_2\left(\psi_{r,rr} + \frac{\psi_{,r}}{r} - \frac{\psi_r}{r^2}\right) = 0 \tag{25}$$

$$\begin{aligned} &K_1\left[\frac{1}{2r}(w_{,r})^3 + \frac{3}{2}w_{,rr}(w_{,r})^2 + w_{,rr}\left(u_{,r} + \frac{\nu}{r}u - \frac{\kappa(1-\nu)}{2}\right) + w_{,r}\left(u_{,rr} + \frac{1+\nu}{r}u_{,r} + \frac{\kappa(1-\nu)}{2r}\right)\right] \\ &\quad + \frac{\kappa(1-\nu)}{2}K_1\left[\frac{1}{r}\psi_r + \psi_{r,r}\right] + K_2\left[w_{,rr}\left(\psi_{r,r} + \frac{\nu}{r}\psi_r\right) + w_{,r}\left(\psi_{r,rr} + \frac{1+\nu}{r}\psi_{r,r}\right)\right] + P(r.t) = I \cdot w_{,tt} \end{aligned} \tag{26}$$

$$-\frac{\kappa(1-\nu)}{2}K_1(w_{,r} + \psi_r) + K_2\left(\frac{(1-\nu)}{2r}(w_{,r})^2 + w_{,rr}w_{,r} + u_{,rr} + \frac{u_{,r}}{r} - \frac{u}{r^2}\right) + K_3\left(\psi_{r,rr} + \frac{\psi_{r,r}}{r} - \frac{\psi_r}{r^2}\right) = 0 \tag{27}$$

Eqs. (25), (26) and (27) are dynamic forms of von-Karman's equations, where the longitudinal and rotary inertias are neglected. Together, they govern the finite-amplitude, axisymmetric vibration of a thick annular or circular plate. These governing differential equations are complicated by the obvious nonlinear coupling of membrane and bending theories for thick plates.

By introducing dimensionless variables as

$$\begin{aligned} &\bar{r} = \frac{r}{r_o}, \quad \bar{h} = \frac{h}{r_o}, \quad \bar{u} = \frac{u}{r_o}, \quad \bar{w} = \frac{w}{r_o}, \\ &\tau = \frac{1}{r_o}\sqrt{\frac{E_m}{\rho_m}}, \quad \bar{\Omega} = r_o\sqrt{\frac{\rho_m}{E_m}}\Omega, \quad p(\bar{r},\tau) = \frac{P(r,t)}{E_m} \end{aligned} \tag{28}$$

and

$$\bar{K}_1 = \frac{K_1}{r_o E_m}, \quad \bar{K}_2 = \frac{K_2}{{r_o}^2 E_m}, \quad \bar{K}_3 = \frac{K_3}{{r_o}^3 E_m}, \quad \bar{I} = \frac{I}{r_o \rho_m} \tag{29}$$

The governing equations can now be written in non-dimensional form by using the above dimensionless variables. In the following equations and relations we eliminate the bar sign for simplicity.

$$K_1\left(\frac{(1-\nu)}{2r}(w_{,r})^2 + w_{,rr}w_{,r} + u_{,rr} + \frac{u_{,r}}{r} - \frac{u}{r^2}\right) + K_2\left(\psi_{r,rr} + \frac{\psi_{,r}}{r} - \frac{\psi_r}{r^2}\right) = 0 \tag{30}$$

$$K_1\left[\frac{1}{2r}\left(w_{,r}\right)^3+\frac{3}{2}w_{,rr}\left(w_{,r}\right)^2+w_{,rr}\left(u_{,r}+\frac{\nu}{r}u-\frac{\kappa(1-\nu)}{2}\right)+w_{,r}\left(u_{,rr}+\frac{1+\nu}{r}u_{,r}+\frac{\kappa(1-\nu)}{2r}\right)\right]$$
$$+\frac{\kappa(1-\nu)}{2}K_1\left[\frac{1}{r}\psi_r+\psi_{r,r}\right]+K_2\left[w_{,rr}\left(\psi_{r,r}+\frac{\nu}{r}\psi_r\right)+w_{,r}\left(\psi_{r,rr}+\frac{1+\nu}{r}\psi_{r,r}\right)\right]+p(r.\tau)=I\cdot w_{,\tau\tau} \quad (31)$$

$$-\frac{\kappa(1-\nu)}{2}K_1(w_{,r}+\psi_r)+K_2\left(\frac{(1-\nu)}{2r}(w_{,r})^2+w_{,rr}w_{,r}+u_{,rr}+\frac{u_{,r}}{r}-\frac{u}{r^2}\right)+K_3\left(\psi_{r,rr}+\frac{\psi_{r,r}}{r}-\frac{\psi_r}{r^2}\right)=0 \quad (32)$$

In order to solve governing Eqs. (30), (31) and (32), they must be accompanied by a set of boundary conditions at both inner and outer boundary for any time τ. It is assumed that the plate is immovably clamped in both inner and outer radius. The boundary conditions are

Inner radius: $w(r_i,\tau)=0,\quad u(r_i,\tau)=0,\quad \psi_r(r_i,\tau)=0$ (33)

Outer radius: $w(r_o,\tau)=0,\quad u(r_o,\tau)=0,\quad \psi_r(r_o,\tau)=0$ (34)

3 METHOD OF SOLUTION

In spite of many researches about the study of the nonlinear behavior of plates, there is still no analytical solution for Eqs. (30), (31) and (32). The reason is in coupling nature of governing equations as well as the non-linear terms of the derivatives of the displacements. In the analysis and solution of this kind of equations two approximate methods are commonly used. One is known as *"assumed-space-mode"* solution, generally, which is achieved by taking some assumed spatial shape functions and by using a variational method to eliminate the spatial variables and reduce the partial differential equations to ordinary ones only including time as independent variable [19, 22]. Another method is *"assumed-time-mode"* solution. Upon assuming an appropriate harmonic response for the non-linear vibrations, the time variable is eliminated by using a Kantorovich averaging method [5, 23, 24] and a non-linear boundary value problem is obtained including spatial variables. This boundary value problem is solved numerically. In the present investigation, the latter method is employed.

3.1 Kantorovich averaging method

Firstly, it is assumed the plate is imposed by a harmonic load with the following form

$$p(r,\tau)=F(r)\sin\Omega\tau \quad (35)$$

and for the purpose of the approximate analysis, the steady-state response is assume to be as follows

$$w(r,\tau)=W(r)\sin\Omega\tau \quad (36)$$

$$u(r,\tau)=U(r)\left(\sin\Omega\tau\right)^2 \quad (37)$$

$$\psi_r(r,\tau)=\Psi_r(r)\sin\Omega\tau \quad (38)$$

where Ω is the non-dimensional frequency of the system, $W(r)$, $U(r)$ and $\Psi(r)$ are the shape functions corresponding to displacement W, U and Ψ respectively. Assumption (37) for $U(r)$ is consistent with the fact that the radial displacement of any point of the plate is independent of the up or down position of the plate. Since expressions (35) - (38) can not satisfy Eqs. (30), (31) and (32) for all τ, the following integrals are employed to obtain equations which can approximate the governing equations within the limits of the assumed form of motion as given in Eqs. (35) - (38).

$$A^* = \int_{r_i}^{r_o}\left[K_1\left(\frac{(1-\nu)}{2r}(w_{,r})^2 + w_{,rr}w_{,r} + u_{,rr} + \frac{u_{,r}}{r} - \frac{u}{r^2}\right) + K_2\left(\psi_{r,rr} + \frac{\psi_{,r}}{r} - \frac{\psi_r}{r^2}\right)\right]\delta u(2\pi r)\mathrm{d}r \tag{39}$$

$$B^* = \int_{r_i}^{r_o}\left[K_1\left(\frac{1}{2r}(w_{,r})^3 + \frac{3}{2}w_{,rr}(w_{,r})^2 + w_{,rr}\left(u_{,r} + \frac{\nu}{r}u - \frac{\kappa(1-\nu)}{2}\right)\right) - K_1\left(w_{,r}\left(u_{,rr} + \frac{1+\nu}{r}u_{,r} + \frac{\kappa(1-\nu)}{2r}\right)\right)\right.$$
$$\left. + \frac{\kappa(1-\nu)}{2}K_1\left(\frac{1}{r}\psi_r + \psi_{r,r}\right) + K_2\left(w_{,rr}\left(\psi_{r,r} + \frac{\nu}{r}\psi_r\right) + w_{,r}\left(\psi_{r,rr} + \frac{1+\nu}{r}\psi_{r,r}\right)\right) + p(r.\tau) - I\cdot w_{,\tau\tau}\right]\delta w(2\pi r)\ \mathrm{d}r \tag{40}$$

$$C^* = \int_{r_i}^{r_o}\left[-\frac{\kappa(1-\nu)}{2}K_1(w_{,r} + \psi_r) + K_2\left(\frac{(1-\nu)}{2r}(w_{,r})^2 + w_{,rr}w_{,r} + u_{,rr} + \frac{u_{,r}}{r} - \frac{u}{r^2}\right)\right.$$
$$\left. + K_3\left(\psi_{r,rr} + \frac{\psi_{r,r}}{r} - \frac{\psi_r}{r^2}\right)\right]\delta\psi_r(2\pi r)\mathrm{d}r \tag{41}$$

in which

$$\delta w = \delta W\sin\Omega\tau \qquad \delta u = \delta U(\sin\Omega\tau)^2 \qquad \delta\psi_r = \delta\Psi_r\sin\Omega\tau \tag{42}$$

For any instant, the relations (39), (40) and (41) is equal to the virtual work of all the membrane forces, transverse forces and bending moments as they move through a virtual displacement δu, δw and $\delta\psi_r$. Equating the average virtual work over one period oscillation to zero,

$$A = \int_0^{2\pi/\Omega} A^*\mathrm{d}\tau = 0 \tag{43}$$

$$B = \int_0^{2\pi/\Omega} B^*\mathrm{d}\tau = 0 \tag{44}$$

$$C = \int_0^{2\pi/\Omega} C^*\mathrm{d}\tau = 0 \tag{45}$$

yields

$$\frac{(1-\nu)}{2r}(W_{,r})^2 + W_{,rr}W_{,r} + U_{,rr} + \frac{U_{,r}}{r} - \frac{U}{r^2} = 0 \tag{46}$$

$$K_1\left[\frac{3}{8r}(W_{,r})^3 + \frac{9}{8}W_{,rr}(W_{,r})^2 + W_{,rr}\left(\frac{3}{4}U_{,r} + \frac{3\nu}{4r}U - \frac{\kappa(1-\nu)}{2}\right) - W_{,r}\left(\frac{3}{4}U_{,rr} + \frac{3(1+\nu)}{4r}U_{,r} + \frac{\kappa(1-\nu)}{2r}\right)\right]$$
$$+ \frac{\kappa(1-\nu)}{2}K_1\left(\frac{1}{r}\Psi_r + \Psi_{r,r}\right) + F(r) + I\cdot\Omega^2\cdot W = 0 \tag{47}$$

$$-\frac{\kappa(1-\nu)}{2}K_1(W_{,r} + \Psi_r) + K_3\left(\Psi_{r,rr} + \frac{\Psi_{r,r}}{r} - \frac{\Psi_r}{r^2}\right) = 0 \tag{48}$$

Set of Eqs. (46), (47) and (48) along with boundary conditions (33) and (34) compose the two-point nonlinear boundary value problem which governs the large amplitude vibration of a thick annular FGM plate.

3.2 Shooting method for boundary value problem

Since it is difficult to analytically solve the boundary value problem of Eqs. (46), (47) and (48), shooting method or trial and error method [5, 23, 24] is employed to get a numerical solution of the nonlinear two point boundary-value problem. First the higher order equations must be rewritten as a coupled set of first-order equations

$$\mathrm{M}(r,\mathrm{Y})\left\{\frac{\mathrm{dY}}{\mathrm{d}r}\right\}=\mathrm{H}(r,\mathrm{Y},F),\qquad a\le r\le 1,\qquad a=r_i/r_o \tag{49}$$

$$\mathbf{B_1}\mathbf{Y}(a)=\{0,0,0\}^{\mathbf{T}} \tag{50a}$$

$$\mathbf{B_2}\mathbf{Y}(1)=\{0,0,0\}^{\mathbf{T}} \tag{50b}$$

where

$$\mathbf{Y}=\{y_1\quad y_2\quad y_3\quad y_4\quad y_5\quad y_6\}^{\mathbf{T}}=\{W\quad U\quad \Psi_r\quad W_{,r}\quad U_{,r}\quad \Psi_{r,r}\}^{\mathbf{T}} \tag{51}$$

$$\mathbf{M}=\begin{bmatrix}1&0&0&0&0&0\\0&1&0&0&0&0\\0&0&1&0&0&0\\0&0&0&y_4&1&0\\0&0&0&m_{54}&3K_1y_4/4&0\\0&0&0&0&0&K_3\end{bmatrix} \tag{52a}$$

$$\mathbf{H}=\{y_4\quad y_5\quad y_6\quad h_4\quad h_5\quad h_6\}^{\mathbf{T}} \tag{52b}$$

in which

$$m_{54}=K_1\left(\frac{3\nu}{4r}+\frac{3}{4}y_5+\frac{\kappa(1-\nu)}{2}+\frac{9}{8}y_4^2\right) \tag{53}$$

$$h_4=\frac{y_2}{r^2}-\frac{y_5}{r}-\frac{1-\nu}{2r}y_4^2 \tag{54}$$

$$h_5=-K_1y_4\left(\frac{3(1+\nu)}{4r}y_5+\frac{\kappa(1-\nu)}{2r}\right)-\frac{3}{8r}K_1y_4^3-\frac{\kappa(1-\nu)}{2}K_1y_6-\frac{\kappa(1-\nu)}{2r}K_1y_3-I\cdot\Omega^2\cdot y_1-F \tag{55}$$

$$h_6=y_3\left(\frac{K_3}{r^2}+\frac{\kappa(1-\nu)}{2}K_1\right)-\frac{K_3}{r}y_6-\frac{\kappa(1-\nu)}{2}K_1y_4 \tag{56}$$

$$\mathbf{B_1}=\mathbf{B_2}=\begin{bmatrix}1&0&0&0&0&0&0\\0&1&0&0&0&0&0\\0&0&1&0&0&0&0\end{bmatrix} \tag{57}$$

Let us consider the initial problem corresponding to boundary-value problem (49) and (50)

$$\mathrm{M}(r,\mathrm{Z})\left\{\frac{\mathrm{dZ}}{\mathrm{d}r}\right\}=\mathrm{H}(r,\mathrm{Z},F),\qquad a\le r \tag{58}$$

$$\mathbf{Z}(a)=\{0\quad 0\quad 0\quad x_1\quad x_2\quad x_3\quad x_4\}^{\mathbf{T}} \tag{59}$$

where

$$\mathbf{Z} = \{z_1 \quad z_2 \quad z_3 \quad z_4 \quad z_5 \quad z_6 \quad z_7\}^{\mathbf{T}}, \qquad \mathbf{X} = \{x_1 \quad x_2 \quad x_3 \quad x_4\}^{\mathbf{T}} \tag{60}$$

$\mathbf{X}$ is an unknown vector related to the missing initial values of $\mathbf{Y}$ at $r = a$. For a prescribe value of Ω, the components of $\mathbf{X}$ are searched for such that solution of initial value problem (58), (59) also satisfies the boundary condition (50b), i.e.,

$$\mathbf{B_2 Z}(1, \Omega, \mathbf{X}^*, F) = \{0, 0, 0\}^{\mathbf{T}} \tag{61}$$

If $\mathbf{X} = \mathbf{X}^*$ is a root of Eq. (61), the solution for the boundary-value problem (49) and (50) is then obtained as

$$\mathbf{Y}(r) = \mathbf{Z}(r, \Omega, \mathbf{X}^*, F) \tag{62}$$

Table 2
Clamped isotropic annular plate with various thickness and inner-outer radius ratios: comparison of the first four linear frequency parameters ω

r_i/r_0	h/r_0	ω_1		ω_2		ω_3		ω_4	
		Present	Han and Liew [25]	Present	Han and Liew [25]	Present	Han and Liew [25]	Present	Han and Liew [25]
0.1	0.05	26.546	26.534	71.232	71.228	135.245	135.24	215.114	215.08
	0.1	24.634	24.629	62.146	62.140	111.127	111.12	167.166	167.16
	0.2	19.852	19.843	44.922	44.913	74.869	74.860	106.815	106.81
0.3	0.05	43.604	43.599	115.272	115.27	214.625	214.62	334.708	334.70
	0.1	39.395	39.389	95.598	95.593	165.267	165.26	242.176	242.17
	0.2	30.046	30.040	64.239	64.232	104.095	104.09	145.236	145.23
0.5	0.05	83.056	83.051	211.98	211.95	381.456	381.45	576.994	576.99
	0.1	70.283	70.277	159.786	159.78	265.445	265.44	378.427	378.42
	0.2	48.317	48.310	97.397	97.389	155.477	155.47	196.796	196.79

Therefore, a harmonic response of Eqs. (30)- (34) is obtained in the form of Eqs. (35)-(38). A relative error limit, $\varepsilon = 10^{-6}$ was taken to warrant that both the numerical integration and the successive correction were carried out until the error norm became less than ε.

4 VERIFICATION OF RESULTS

In order to show the reliability of the numerical technique employed here, we firstly give some numerical tests. The present results are validated by taking the linear and nonlinear steady-state free vibration of circular and annular clamped isotropic plates. Non-dimensional linear natural frequencies of clamped annular plates are given by Eq. (63) [25].

$$\omega = \frac{r_o^2 \Omega}{h} \sqrt{\frac{12(1-\nu^2)\rho_m}{E_m}} \tag{63}$$

Firstly, results for linear natural frequencies of clamped annular isotropic plates for different thickness ratios and inner-to-outer ratios are compared with ones given by Ref. [25]. Three thickness ratios $0.05, 0.1, 0.2$ have been considered. Note that $h/r_o = 0.05$ corresponds to a thin plate; $h/r_o = 0.1$ correspond to moderately thick plates

whereas $h/r_o = 0.2$ corresponds to a thick plate. Table 2 shows the results of present study and those of Ref. [25]. Good agreement has been observed for all cases ranging from very thin to very thick cases.

Secondly, consider a circular plate with $h/r_o = 0.04$. Fig. 2 shows the nonlinear normalized fundamental mode shapes $W(r)/W_{max}$ of a clamped immovable circular metallic plate for two non-dimensional amplitudes of axisymmetric vibration W_{max}/h =0.5 and W_{max}/h =2. The results are in good agreement with those given in Ref. [26]. Thirdly, the first nonlinear normalized axisymmetric mode shapes of a clamped immovable FGM circular metallic plate for various values of g at W_{max}/h=2 are plotted in Fig. 3 and are compared with those of Ref. [23]. The close agreement between the results of this study and the results of Ref. [23] can be observed. Based on the presented comparison studies, we can warrant that the present approach can yield accurate solutions.

5 NUMERICAL RESULTS AND DISCUSSIONS

Numerical results are presented in this section for FGM plates with two constituent materials. The material properties of the FGM constituents are listed in Table 1. A program was developed for the purpose and many examples have been solved numerically, including the following. Throughout the following computation, let $r_i/r_o = 0.3$, $h/r_o = 0.1$ and $\nu = 0.3$. Figs. 4(a) and (b) depict the variation of the dimensionless radial stress with dimensionless vibration amplitude, and on ceramic-rich surface for the different values of g respectively at inner (r=0.3) and outer (r=1) radius. For the low vibration amplitudes, variation of g has no considerable effect on stresses, while for higher values of vibration amplitude; the effect of variation of gradient index g on stresses is more significant. Figs. 5(a), (b) and 6(a), (b) show, respectively, the variation of the dimensionless circumferential and shear stresses with dimensionless vibration amplitude on ceramic-rich surface for the different values of g at inner and outer radius.

Figs. 7, 8, and 9 highlight the influence of g on the variation of the dimensionless radial, circumferential and shear stresses along dimensionless radius on metal-rich surface at W_{max}/h=1. Due to the curvature of the plate in the first mode on z= -0.5, the normal stresses are negative in r= $(r_o+r_i)/2$ and positive in both clamped edges of the plate. While the shear stresses are positive and negative at inner and outer radii respectively, it shows a minuscule amount at r= $(r_o+r_i)/2$.

Relationship of the dimensionless radial, circumferential and shear stresses with dimensionless thickness of the plate for different values of g at r=1 and W_{max}/h=1 are depicted in Figs. 10, 11 and 12 respectively. It is obvious that with increasing g, the amount of stresses decrease. For ceramic-rich and metal-rich surfaces (g = 0 and g>>10), the stress distribution is linear, where for the FGM plate, the behavior is nonlinear and is governed by the variation of the properties in the thickness direction. One of the most significant points of these figures is that the neutral plane of the plate is not conforming to the mid-plane in this case. It is clear that the Young's modulus of the ceramic is greater than the metal, so the neutral plane is near by the ceramic-rich surface.

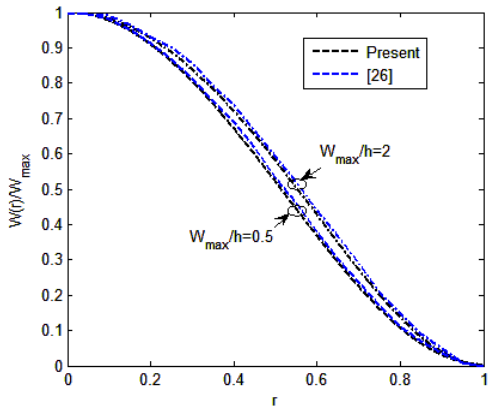

Fig 2.
Normalized nonlinear fundamental mode shape $W(r)/W_{max}$ a clamped immovable circular metallic plate for various nondimensional vibration amplitudes.

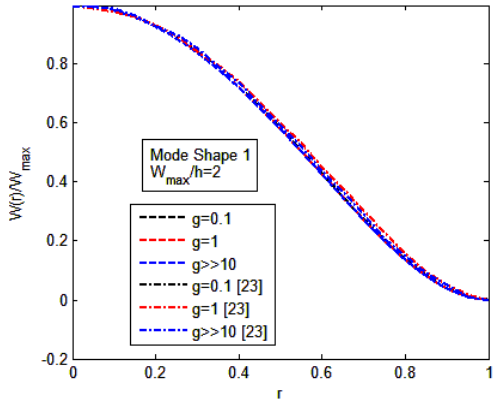

Fig 3.
First nonlinear normalized axisymmetric mode shapes of the clamped circular functionally graded plate for different values of *g*.

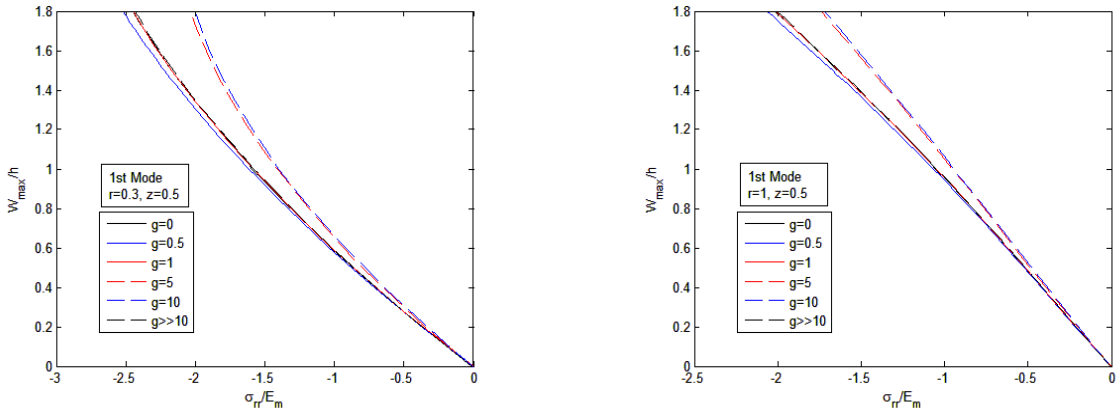

(a) (b)

Fig 4.
Variation of the dimensionless radial stress with dimensionless vibration amplitude on ceramic-rich surface at (a): inner and (b): outer radius.

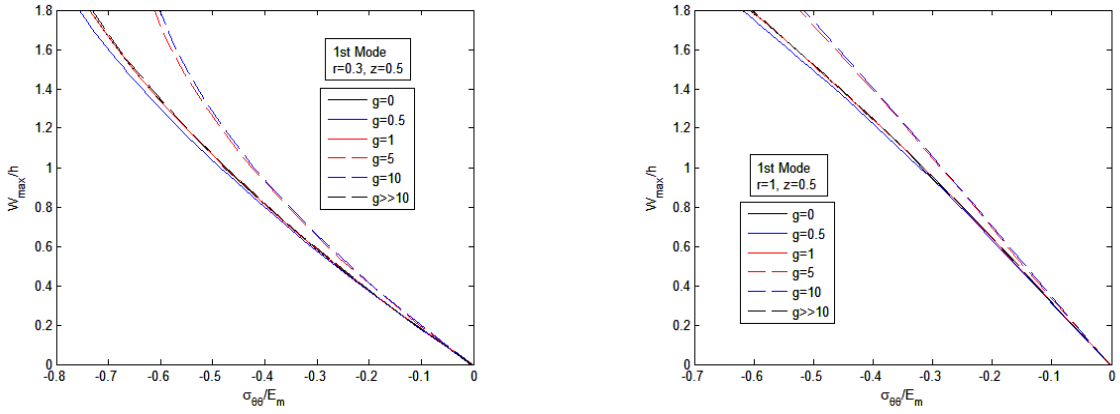

(a) (b)

Fig 5.
Variation of the dimensionless circumferntial stress with dimensionless vibration amplitude on ceramic-rich surface at (a) inner and (b) outer radius.

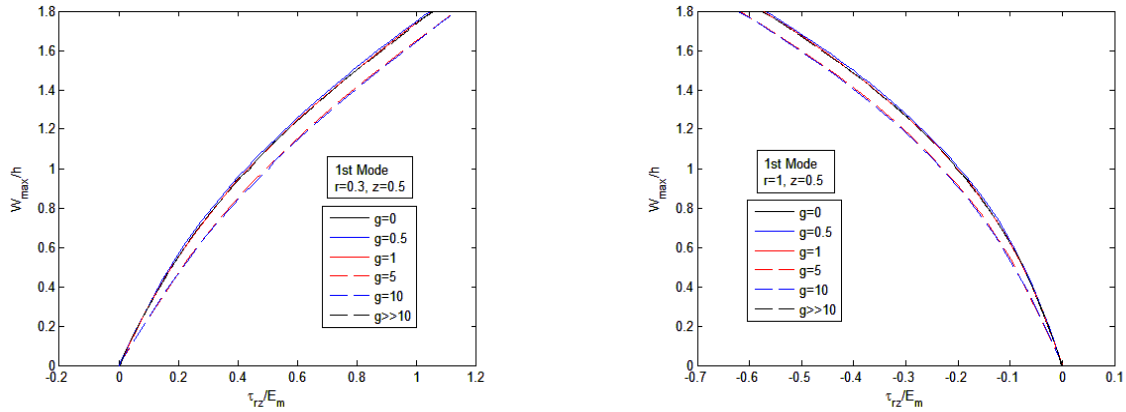

(a) (b)

Fig 6.
Variation of the dimensionless shear stress with dimensionless vibration amplitude on ceramic-rich surface at (a) inner and (b) outer radius.

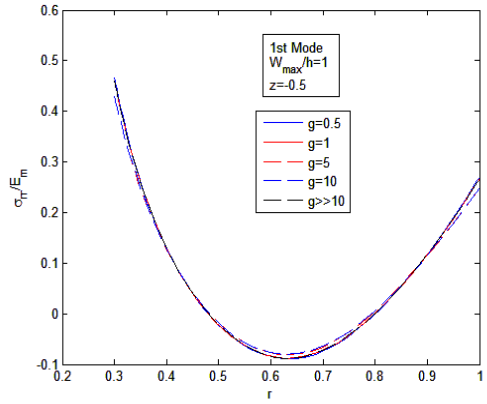

Fig 7.
Variation of the dimensionless radial stress with dimensionless radius on metal-rich surface.

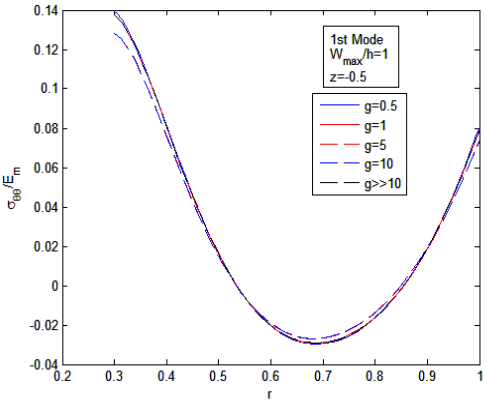

Fig 8.
Variation of the dimensionless circumferential stress with dimensionless radius on metal-rich surface.

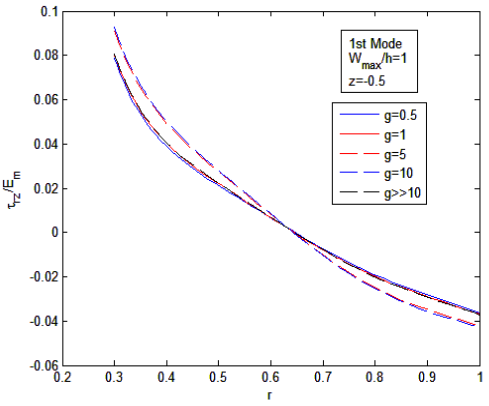

Fig 9.
Variation of the dimensionless shear stress with dimensionless radius on metal-rich surface.

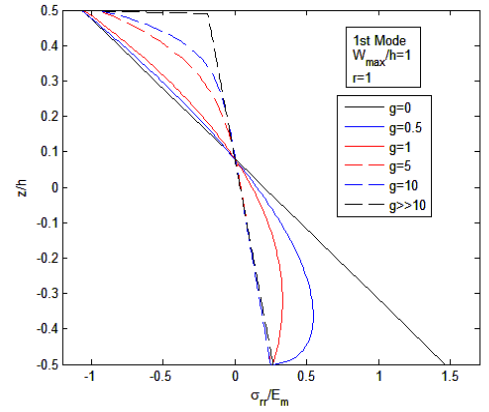

Fig 10.
Variation of the dimensionless radial stress along the thickness of the plate at outer radius.

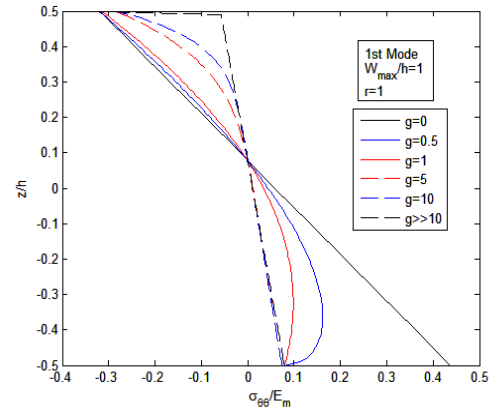

Fig 11.
Variation of the dimensionless circumferential stress along the thickness of the plate at outer radius.

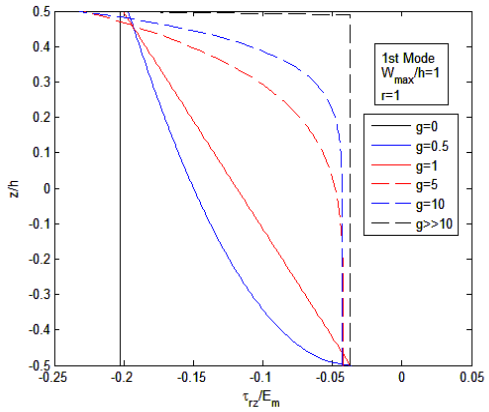

Fig 12.
Variation of the dimensionless shear stress along the thickness of the plate at outer radius.

6 CONCLUDING REMARKS

Large amplitude vibration of a thick annular functionally graded plate has been investigated in this paper by using the first-order shear deformation plate theory and von-Karman-type equation. In the results, the influences of vibration amplitude and volume fraction index on stresses have been examined. For the low vibration amplitudes, variation of volume fraction index has no significant effect on the stresses, but different values of volume fraction index have considerable effect in the amount of stresses in high vibration amplitudes. For ceramic-rich and metal-rich surfaces, the stress distribution in any arbitrary transverse section is linear, where for the FGM plate; the behavior is nonlinear and mid plane of the plate is different from the neutral surface. Comparing shear stress with radial or circumferential stresses concludes that for plates with large thickness ratio (h/r_o) the shear stress is considerable and cannot be neglected in computing total stress.

7 APPENDIX A

Definition of variables K_1, K_2, K_3 and I

$$K_1 = \int_{-h/2}^{h/2} \frac{E(z)}{1-\nu^2}\mathrm{d}z = \frac{h}{1-\nu^2}\frac{E_m(g+1)+E_{cm}}{g+1}$$
$$K_2 = \int_{-h/2}^{h/2} \frac{zE(z)}{1-\nu^2}\mathrm{d}z = \frac{h^2}{2(1-\nu^2)}\frac{gE_{cm}}{(g+1)(g+2)}$$
$$K_3 = \int_{-h/2}^{h/2} \frac{z^2E(z)}{1-\nu^2}\mathrm{d}z = \frac{h^3}{12(1-\nu^2)}\left(E_m + \frac{3E_{cm}(g^2+g+2)}{(g+1)(g+2)(g+3)}\right)$$
$$I = \int_{-h/2}^{h/2} \rho(z)\mathrm{d}z = h\frac{\rho_m(g+1)+\rho_{cm}}{g+1} \qquad \text{(A.1)}$$

in which

$$E_{cm} = E_c - E_m$$
$$\rho_{cm} = \rho_c - \rho_m \qquad \text{(A.2)}$$

REFERENCES

[1] Bhimaraddi A., Chandrashekhara K., 1993, Nonlinear vibrations of heated antisymmetric angle-ply laminated plates, *International Journal of Solids and Structures* **30**: 1255-1268.
[2] Liew K.M., Xiang Y., Kitipornchai S., 1994, Transverse vibration of thick rectangular plates-IV: influence of isotropic in-plane pressure, *Computers and Structures* **49**: 69-78.
[3] Liu F.L., Liew K.M., 1999, Analysis of vibrating thick rectangular plates with mixed boundary constraints using differential quadrature element method, *Journal of Sound and Vibration* **225**: 915-934.
[4] Shen H.S., Yang J., Zhang L., 2000, Dynamic response of Reissner-Mindlin plates under thermomechanical loading and resting on elastic foundations, *Journal of Sound and Vibration* **232**: 309-329.
[5] Li S.R., Zhou Y.H., Song X., 2002, Non-linear vibration and thermal buckling of an orthotropic annular plate with a centric rigid mass, *Journal of Sound and Vibration* **251**: 141-152.
[6] Ebrahimi F., Rastgoo A., 2008, Free vibration analysis of smart annular FGM plates integrated with piezoelectric layers, *Smart Materials and Structures*, doi:10.1088/0964-1726/17/1/015044.
[7] Xuefeng S., Xiaoqing Z., Jinxiang Z., 2000, Thermoelastic free vibration of clamped circular plate, *Applied Mathematics and Mechanics* **21**: 715-724.
[8] Arafat H.N., Nayfeh A.H., Faris W., 2004: Natural frequencies of heated annular and circular plates, *International Journal of Solids and Structures* **41**: 3031-3051.
[9] Amini M.H., Soleimani M., Rastgoo A., 2009, Three-dimensional free vibration analysis of functionally graded material plates resting on an elastic foundation, *Smart Materials and Structures*, doi:10.1088/0964-1726/18/8/085015.
[10] Ebrahimi F., Rastgoo A., Atai A.A., 2008, A theoretical analysis of smart moderately thick shear deformable annular functionally graded plate, *European Journal of Mechanics A/Solids*, doi: 10.1016/j.euromechsol.2008.12.008.
[11] Praveen G.N., Reddy J.N., 1998, Nonlinear transient thermoelastic analysis of functionally graded ceramic-metal plates, *International Journal of Solids and Structures* **35**: 4457-4476.
[12] Reddy J.N., 2000, Analysis of functionally graded plates, *International Journal of Numerical Methods in Engineering* **47**: 663-684.
[13] Woo J., Meguid S.A., 2001, Nonlinear analysis of functionally graded plates and shallow shells, *International Journal of Solids and Structures* **38**: 7409-7421.
[14] Woo J., Meguid S.A., Ong L.S., 2006, Nonlinear free vibration behavior of functionally graded plates, *Journal of Sound and Vibration* **289**: 595-611.
[15] Allahverdizadeh A., Naei M.H., Ratgo A., 2006, The effects of large vibration amplitudes on the stresses of thin circular functionally graded plates, *International Journal of Mechanics and Materials in Design* **3**: 161-174.
[16] Kitipornchai S, Yang J., Liew K.M., 2004, Semi-analytical solution for nonlinear vibration of laminated FGM plates with geometric imperfections, *International Journal of Solids and Structures* **41**: 2235-2257.
[17] Kitipornchai S., Yang J., Liew K.M., 2006, Random vibration of the functionally graded laminates in thermal environments, *Computer Methods in Applied Mechanics and Engineering* **195**: 1075-1095.
[18] Shafiee H., Naei M.H., Eslami M.R., 2006, In-plane and out-of-plane buckling of arches made of FGM, *International Journal of Mechanical Sciences* **48**: 907-915.
[19] Huang X.L., Shen H.S., 2004, Nonlinear vibration and dynamic response of functionally graded plates in thermal environments, *International Journal of Solids and Structures* **41**: 2403-2427.
[20] Mindlin R.D., 1951, Influence of rotary inertia and shear on flexural motions of isotropic elastic plates, *Journal of Applied Mechanics* **18**: 31-8.
[21] Reddy J.N., 1999, *Theory and Analysis of Elastic Plates, Taylor and Francis*, Philadelphia.
[22] Huang S., 1998, Non-linear vibration of a hinged orthotropic circular plate with a concentric rigid mass, *Journal of Sound and Vibration* **214**: 873-883.
[23] Allahverdizadeh A., Naei M.H., Nikkhah Bahrami M., 2008, Nonlinear free and forced vibration analysis of thin circular functionally graded plates, *Journal of Sound and Vibration* **310**: 966-984.
[24] Ma L.S., Wang T.J., 2003, Nonlinear bending and post-buckling of a functionally graded circular plate under mechanical and thermal loadings, *International Journal of Solids and Structures* **40**: 3311-3330.
[25] Han J.B,, Liew K.M., 1999, Axisymmetric free vibration of thick annular plates, *International Journal of Mechanical Sciences* **41**: 1089-1109.
[26] Haterbouch M.,, Benamar R., 2004, The effects of large vibration amplitudes on the axisymmetric mode shapes and natural frequencies of clamped thin isotropic circular plates, part II: iterative and explicit analytical solution for non-linear coupled transverse and in-plane vibrations, *Journal of Sound and Vibration* **277**: 1-30.